Universidade de São Paulo
Instituto de Ciências Matemáticas
e de Computação

Mathematical modeling of micro-textured lubricated contacts

Alfredo Jaramillo
Advisor: Prof. Dr. Gustavo Buscaglia

May 27, 2015

An example of a tribological mechanism

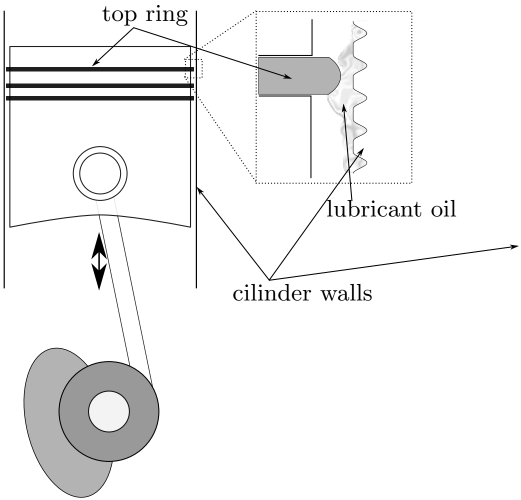

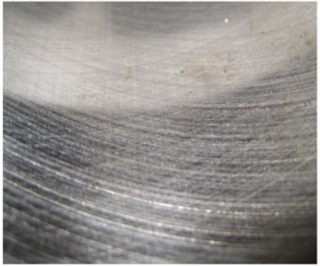

Figure : Scheme of a combustion engine piston; textured liner picture by Guo et al., 2013.

Experimental example

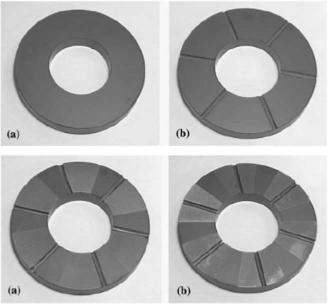

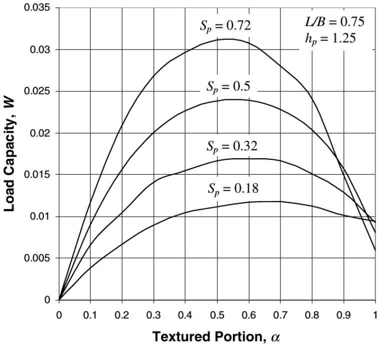

Figure : Left: contacts considered by Etsion et al. (2004). Right: Dependency of the *Load Capacity* upon texture the texture density S_p and the total textured area α. *Friction Coefficient* and *Minimum Clearance* dependencies were also obtained. Brizmer et al. (2003).

Energy losses

Around 5% of the energy losses in a passengers car is to friction in the Piston Rings of the engine (Holmberg et al., 2012).

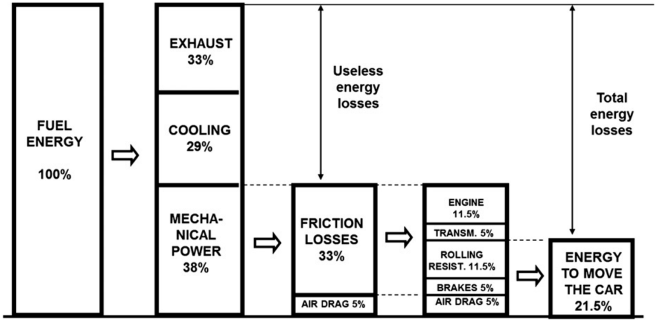

Figure : Diagram of energy losses in a passengers car.

Asymptotic expansion of Navier-Stokes equations

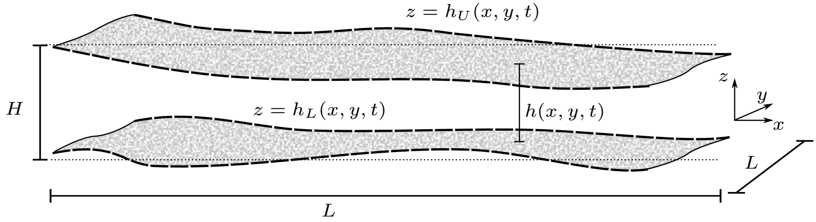

Proximity Hypothesis

The hydrodynamics of a fluid between two surfaces near each other ($\epsilon = H/L \ll 1$) can be modeled by Reynolds equation (e.g., Cameron, 1971).

$$\rho \left(\frac{\partial \vec{\mathbf{u}}}{\partial t} + (\vec{\mathbf{u}} \cdot \nabla) \vec{\mathbf{u}} \right) = -\nabla p + \mu \nabla^2 \vec{\mathbf{u}},$$

$$\hat{x} = \frac{x}{L}, \hat{y} = \frac{y}{L}, \hat{z} = \frac{z}{H}, \qquad \hat{u} = \frac{u}{U}, \hat{v} = \frac{v}{U}, \hat{w} = \frac{w}{U\frac{H}{L}}, \qquad \hat{t} = \frac{t\,U}{L}, \hat{p} = p\frac{H^2}{\mu L\,U},$$

Neglecting terms

Reynolds Number: $\mathrm{Re} = \dfrac{\text{inertia}}{\text{viscous}} = \rho U H/\mu$

$$\frac{\partial \hat{p}}{\partial \hat{x}} = \frac{\partial^2 \hat{u}}{\partial \hat{z}^2} - \epsilon\,\mathrm{Re}\left(\frac{\partial \hat{u}}{\partial \hat{t}} + \hat{u}\frac{\partial \hat{u}}{\partial \hat{x}} + \hat{v}\frac{\partial \hat{u}}{\partial \hat{y}} + \hat{w}\frac{\partial \hat{u}}{\partial \hat{z}}\right) + \mathcal{O}\left(\epsilon^2\right),$$

$$\frac{\partial \hat{p}}{\partial \hat{y}} = \frac{\partial^2 \hat{v}}{\partial \hat{z}^2} - \epsilon\,\mathrm{Re}\left(\frac{\partial \hat{v}}{\partial \hat{t}} + \hat{u}\frac{\partial \hat{v}}{\partial \hat{x}} + \hat{v}\frac{\partial \hat{v}}{\partial \hat{y}} + \hat{w}\frac{\partial \hat{v}}{\partial \hat{z}}\right) + \mathcal{O}\left(\epsilon^2\right),$$

$$\frac{\partial \hat{p}}{\partial \hat{z}} = -\epsilon^3\,\mathrm{Re}\left(\frac{\partial \hat{w}}{\partial \hat{t}} + \hat{u}\frac{\partial \hat{w}}{\partial \hat{x}} + \hat{v}\frac{\partial \hat{w}}{\partial \hat{y}} + \hat{w}\frac{\partial \hat{w}}{\partial \hat{z}}\right) + \mathcal{O}(\epsilon^2).$$

Reynolds equation

$$\nabla \cdot \vec{\mathbf{u}} = 0 \Rightarrow \frac{\partial}{\partial x}\left(\frac{h^3}{12\,\mu}\frac{\partial p}{\partial x} - \overline{U}h\right) + \frac{\partial}{\partial y}\left(\frac{h^3}{12\,\mu}\frac{\partial p}{\partial y} - \overline{V}h\right) = \frac{\partial h}{\partial t},$$

where $\overline{U} = \frac{U_L + U_H}{2}$ and $\overline{V} = \frac{V_L + V_H}{2}$. First studied by Osborne Reynolds (1886).

Friction formula

Constitutive relation for Newtonian Fluids

$$\tau_{ij} = -p\,\delta_{ij} + \mu\left(\frac{\partial u_i}{\partial x_j} + \frac{\partial u_j}{\partial x_i}\right).$$

Proximity Hypothesis

$$d\hat{f} = \boldsymbol{\tau}\cdot\hat{\boldsymbol{\imath}}\cdot d\boldsymbol{S},$$

$$= \mu\frac{U}{H}\left(\hat{p}\frac{\partial \hat{h}_L}{\partial \hat{x}} - 2\epsilon^2\frac{\partial \hat{u}}{\partial \hat{x}}\frac{\partial \hat{h}_L}{\partial \hat{x}} - \epsilon^2\left(\frac{\partial \hat{u}}{\partial \hat{y}} + \frac{\partial \hat{v}}{\partial \hat{x}}\right)\frac{\partial \hat{h}_L}{\partial \hat{y}} + \frac{\partial \hat{u}}{\partial \hat{z}} + \epsilon\frac{\partial \hat{w}}{\partial \hat{x}}\right)L^2 d\hat{x}d\hat{y},$$

$$f \approx \int_\Omega\left(p\frac{\partial h_L}{\partial x} - \frac{h}{2}\frac{\partial p}{\partial x} - \mu\frac{(U_L - U_H)}{h}\right)dx\,dy.$$

Friction formula

Constitutive relation for Newtonian Fluids

$$\tau_{ij} = -p\,\delta_{ij} + \mu\left(\frac{\partial u_i}{\partial x_j} + \frac{\partial u_j}{\partial x_i}\right).$$

Proximity Hypothesis

$$d\hat{f} = \boldsymbol{\tau}\cdot\hat{\boldsymbol{\imath}}\cdot d\boldsymbol{S},$$

$$= \mu\frac{U}{H}\left(\hat{p}\frac{\partial\hat{h}_L}{\partial\hat{x}} - 2\epsilon^2\frac{\partial\hat{u}}{\partial\hat{x}}\frac{\partial\hat{h}_L}{\partial\hat{x}} - \epsilon^2\left(\frac{\partial\hat{u}}{\partial\hat{y}} + \frac{\partial\hat{v}}{\partial\hat{x}}\right)\frac{\partial\hat{h}_L}{\partial\hat{y}} + \frac{\partial\hat{u}}{\partial\hat{z}} + \epsilon\frac{\partial\hat{w}}{\partial\hat{x}}\right)L^2 d\hat{x}d\hat{y},$$

$$f \approx \int_\Omega \left(p\frac{\partial h_L}{\partial x} - \frac{h}{2}\frac{\partial p}{\partial x} - \mu\frac{(U_L - U_H)}{h}\right)dx\,dy.$$

Friction from Navier-Stokes and Reynolds equations

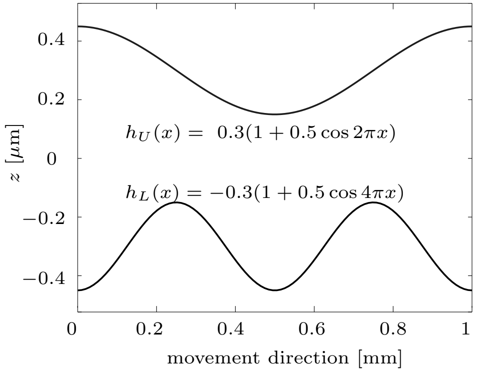

Figure : Sinusoidal surfaces for testing friction formulas.

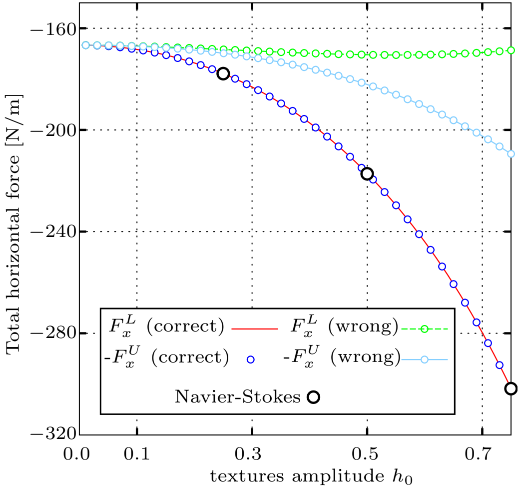

Figure : Total friction (in x) for different friction formulas.

Convergence of the Stokes system

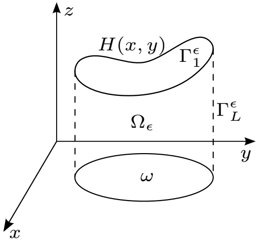

Figure : Adapted: Bayada et al. (1986).

$$-\mu\nabla^2 \mathbf{U}^\epsilon + \nabla p^\epsilon = 0 \qquad (1)$$

$$\nabla\cdot\mathbf{U}^\epsilon = 0. \qquad (2)$$

Suppose $\exists g^\epsilon \in H^{1/2}(\Gamma^\epsilon)$ s.t.

$$\begin{cases} g^\epsilon = 0 & \text{on } \Gamma_1^\epsilon \\ g^\epsilon = S > 0 & \text{on } \omega \\ \int_{\Gamma_L^\epsilon} g^\epsilon \cos(\hat{\boldsymbol{n}}, \hat{\boldsymbol{e}}_1)\, d\sigma = 0 \end{cases} \qquad (3)$$

Theorem

Under conditions (3) the Stokes system (1)-(2) has a unique solution $(\mathbf{U}^\epsilon, p^\epsilon)$ *in* $(H^1(\Omega_\epsilon))^3 \times L_0^2(\Omega_\epsilon)$, *with*

$$\mathbf{U}^\epsilon = (g^\epsilon, 0, 0), \ \text{on } \Gamma^\epsilon.$$

Proved in, e.g., Girault et al., 1981.

Also, $\exists \mathbf{G}^\epsilon \in H^1(\Omega_\epsilon)^3$ s.t.

$$\nabla\cdot\mathbf{G}^\epsilon = 0, \ \mathbf{G}^\epsilon - \mathbf{U}^\epsilon \in (H_0^1(\Omega_\epsilon))^3$$

Theorem

Under conditions (3), suppose there exists a constant K, not depending on ϵ, s.t. G^ϵ satisfies

$$\|\nabla \hat{G}_i^\epsilon\|_{(L^2(\Omega))^3} \leq K, \ i = 1, 2, 3,$$

and there exists a function $\hat{g} \in H^{1/2}(\Gamma)$ that does not depends on ϵ, s.t.

$$g^\epsilon(x, y, z) = \hat{g}(x, y, Z)$$

where $Z = z/\epsilon$. Then, there exist a unique $p^* \in L_0^2(\Omega)$ that lies in $H_0^1(\omega)$ s.t.

- $\epsilon^2 p^\epsilon$, $\epsilon^2 \frac{\partial p^\epsilon}{\partial x}$, $\epsilon^2 \frac{\partial p^\epsilon}{\partial y}$ *and* $\epsilon \frac{\partial p^\epsilon}{\partial Z}$ *converge strongly in* $L^2(\omega)$ *to* p^*, $\frac{\partial p^*}{\partial x}$, $\frac{\partial p^*}{\partial y}$ *and* 0 *resp.*
- p^* *satisfies*

$$\nabla \cdot \left(\frac{h^3}{12\mu} \nabla p^* \right) = \frac{S}{2} \frac{\partial h}{\partial x},$$

which is the Reynolds equation in the steady case with $U_L = S$, $U_H = V_H = V_L = 0$.

This result was proved by Bayada et al. (1986).

Weak formulation for Reynolds equation

Multiplying Reynolds equation by some test function $v \in H_0^1(\omega)$ and integrating by part we arrive to the next weak formulation $\forall t \in [0, \infty)$

$$\int_\omega h^3 \nabla p \nabla v \, dA = \int_\omega h \frac{\partial v}{\partial x} \, dA - 2 \int_\omega v \frac{\partial h}{\partial t} \, dA \qquad \forall v \in H_0^1(\omega), \tag{4}$$

$$B(h; p, v) = \ell(h; v) \qquad \forall v \in H_0^1(\omega). \tag{5}$$

Theorem

Suppose, $\forall t \in [0, \infty)$, $h(\cdot, t) \in L^\infty(\omega)$, $\partial_t h(\cdot, t) \in H^{-1}(\omega)$ and there exists $0 < h_{min}$ s.t. $h_{min} \leq h(x, y, t)$ a.e. in ω. Then, there exists a unique $p \in H_0^1(\omega)$ accomplishing the weak formulation of Reynolds equation given by equation (4).

Proof: As $B(h; \cdot)$ is a bilinear continuous form on $H_0^1(\omega)$ and $\ell(h; \cdot) \in H^{-1}(\omega)$ the result holds by the Lax-Milgram Theorem (see, e.g., Functional Analysis, Sobolev Spaces and Partial Differential Equations, Brezis, 2011.).

Extremal formulation and discretization by Galerkin Methods

$$\text{(DF)} \quad \nabla \cdot \left(h^3 \nabla p\right) = 2\,\partial_t h + S\,\partial_x h$$

$$\text{(WF)} \qquad B(p,v) = \ell(v),\ \forall v \in H_0^1(\omega) \quad \Leftrightarrow \quad \min_{v \in H_0^1(\omega)} J(v) = \frac{1}{2} B(v,v) - \ell(v) \qquad \text{(EF)}$$

$$B(p_h, v_h) = \ell(v_h),\ \forall v_h \in V_h \quad \Leftrightarrow \quad \min_{v_h \in V_h} J(v_h) = \frac{1}{2} B(v_h, v_h) - \ell(v_h)$$

$$\mathbf{A}\,\mathbf{p}_h = \mathbf{f} \quad \Leftrightarrow \quad \min_{v_h \in V_h} J(v_h) = \frac{1}{2} \mathbf{v}_h^\intercal \mathbf{A} \mathbf{v}_h - \mathbf{f}^\intercal \mathbf{v}_h$$

The convergence of these discretization is classical (see, e.g., *The Mathematical Theory of Finite Element Methods*, Brenner et al. (2002)).

But FE do not conserve mass locally. Finite volumes is a good choice as later we have to deal with a hyperbolic PDE.

Finite volume methods

Conservative form

$$\frac{\partial q}{\partial t} = -\nabla \cdot \vec{\mathbf{J}}, \qquad \text{on } \Omega.$$

Reynolds equation: $\vec{\mathbf{J}} \equiv \frac{U}{2} h\hat{\boldsymbol{e}}_1 - \frac{h^3}{2}\nabla p$, $q \equiv h$

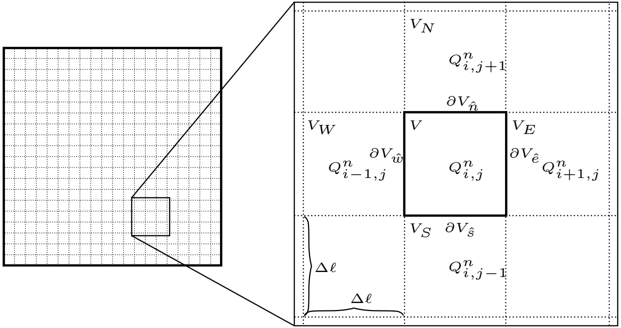

Figure : Finite volumes discretization scheme.

Finite volume methods

Average quantities

$$q_{ij}^n = \frac{1}{|V|}\int_V q(x,y,t_n)\,dv, \qquad J_\xi = \frac{1}{\Delta t}\int_{t_{n-1}}^{t_n}\left(\int_{\partial V_\xi} \vec{\mathbf{J}}\cdot\hat{\boldsymbol{\eta}}\,dl\right)dt.$$

We obtain the equations (exactly satisfied)

$$q_{ij}^n = q_{ij}^{n-1} - \frac{\Delta t}{(\Delta \ell)^2}\left(J_{\hat{n}} - J_{\hat{s}} + J_{\hat{e}} - J_{\hat{w}}\right).$$

So, for the approximated quantities

$$Q_{ij}^n = Q_{ij}^{n-1} - \frac{\Delta t}{(\Delta \ell)^2}\left(\tilde{J}_{\hat{n}} - \tilde{J}_{\hat{s}} + \tilde{J}_{\hat{e}} - \tilde{J}_{\hat{w}}\right),$$

which can be written

$$\mathbf{A}\,\mathbf{p}_h = \mathbf{f} \qquad \Leftrightarrow \qquad \min_{\mathbf{v}_h\in\mathbb{R}^N} \frac{1}{2}\mathbf{v}_h^\intercal \mathbf{A}\mathbf{v}_h - \mathbf{f}^\intercal \mathbf{v}_h$$

1D discretization

Finite Volumes 1D

$$h_i^n = h_i^{n-1} - \frac{\Delta t}{\Delta x}\left(J_x\left(x_{i+\frac{1}{2}}, t_n\right) - J_x\left(x_{i-\frac{1}{2}}, t_n\right)\right)$$

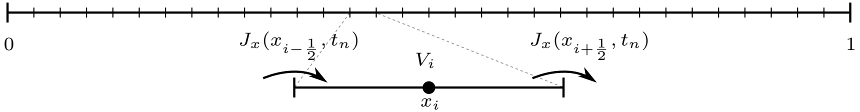

Where $a_{i-1/2} = \frac{\left(h_{i-1}^n\right)^3 + \left(h_i^n\right)^3}{2}$ and we take $\tilde{J}_x\left(x_{i-\frac{1}{2}}, t_n\right) = \frac{S}{2}\, h_{i-1}^n - \frac{1}{2} a_{i-\frac{1}{2}} \frac{P_i^n - P_{i-1}^n}{\Delta x}$.
So we obtain the system

$$a_{i-\frac{1}{2}}^n\, P_{i-1}^n - \left(a_{i-\frac{1}{2}}^n + a_{i+\frac{1}{2}}^n\right) P_i^n + a_{i+\frac{1}{2}}^n\, P_{i+1}^n = f_i^n \qquad \Leftrightarrow \qquad \mathbf{A}\,\mathbf{p}_h^n = \mathbf{f},$$

where $f_i^n = \gamma\left(h_i^n - h_i^{n-1} + \nu\left(h_i^n - h_{i-1}^n\right)\right)$, $\nu = \frac{S}{2}\frac{\Delta t}{\Delta x}$ (Courant number) and $\gamma = 2\,\Delta x^2/\Delta t$.

Pistol Shrimp

https://youtu.be/G_TjlsD1FxA. CC License.

Cavitation in a tribological mechanism

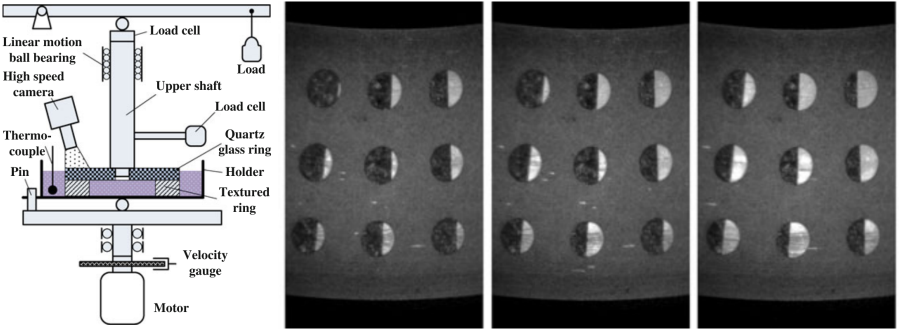

Figure : Cavitation observation in a textured rotating disc. Zhang et al., (2012).

"Direct observation of cavitation phenomenon and hydrodynamic lubrication analysis of textured surfaces", Zhang et al., 2012.

The obstacle problem (OP)

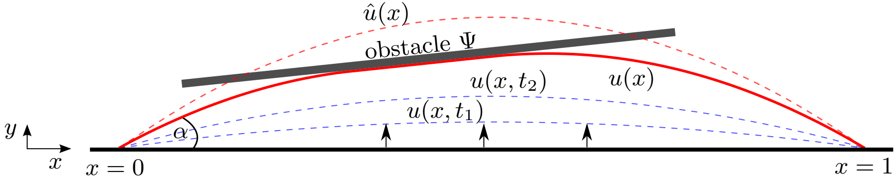

$$\hat{u} \quad \leftrightarrow \quad a(\hat{u}, v) = g(v), \quad \forall v \in H_0^1(0,1)$$

$$u \quad \leftrightarrow \quad a(u, v-u) \geq g(v-u), \quad \forall v \in K_\Psi$$

where $K_\Psi = \{v \in H_0^1(0,1) : v \leq \Psi\}$, a is a continuous bilinear form on $H_0^1(0,1)$ and $g \in H^{-1}(0,1)$. The solution for the inequality exists and it is unique by the Stampacchia Theorem (e.g., *An Introduction to Variational Inequalities and Their Applications*, Kinderlehrer et al., 1980).

Extremal formulation associated and discretization for Reynolds cavitation model

$$\text{(DF)}\ \nabla\cdot\left(h^3\nabla p\right) = 2\,\partial_t h + S\,\partial_x h,\ \text{ in } \omega = \{p>0\}$$

$$\text{(WF)}\ B(p, v-p) \geq \ell(v-p),\ \forall v \in K \quad \Leftrightarrow \quad \min_{v\in K} J(v) = \frac{1}{2}B(v,v) - \ell(v) \quad \text{(EF)}$$

$$B(p_h, v_h - p_h) \geq \ell(v_h - p_h),\ \forall v_h \in K_h \quad \Leftrightarrow \quad \min_{v_h\in K_h} J(v_h) = \frac{1}{2}B(v_h,v_h) - \ell(v_h)$$

$$\mathbf{p}_h^\intercal \mathbf{A}(\mathbf{v}_h - \mathbf{p}_h) \geq \mathbf{f}^\intercal(\mathbf{v}_h - \mathbf{p}_h), \forall \mathbf{v}_h \in \mathbb{R}^N_+ \quad \Leftrightarrow \quad \min_{\mathbf{v}_h\in\mathbb{R}^N_+} J(v_h) = \frac{1}{2}\mathbf{v}_h^\intercal \mathbf{A}\mathbf{v}_h - \mathbf{f}^\intercal \mathbf{v}_h$$

where $K = \{v \in H^1_0(0,1) : v \geq 0\}$.

We have: $\mathbf{p}_h \geq 0 : \mathbf{p}_h^\intercal \mathbf{A}(\mathbf{v}_h - \mathbf{p}_h) \geq \mathbf{f}^\intercal(\mathbf{v}_h - \mathbf{p}_h), \forall \mathbf{v}_h \in \mathbb{R}^N_+ \Leftrightarrow \begin{cases} \mathbf{A}\mathbf{p}_h \geq \mathbf{f} \\ \mathbf{p}_h^\intercal\left(\mathbf{A}\mathbf{p}_h - \mathbf{f}\right) = 0 \\ \mathbf{p}_h \geq 0 \end{cases}$

Convergence of Finite Elements

Theorem

For a triangulation s.t. the angles of the triangles are uniformly bounded below by some positive constant; then, as $h \to 0$, the solution p_h of the problem

$$\min_{v_h \in K_h} J(v_h) = \frac{1}{2} B(v_h, v_h) - \ell(v_h)$$

converges strongly in $H_0^1(\Omega)$ to the solution of the problem

$$\min_{v \in K} J(v) = \frac{1}{2} B(v, v) - \ell(v)$$

where K_h are classical approximations of K by polynomials of degree less than or equal to 1 or 2.

The proof of this theorem can be found in "Lectures on Numerical Methods For Non-Linear Variational Problems", Glowinski (1980).

Convergence of Finite Volumes

SIAM J. Numer. Anal.
Vol. 40, No. 6, pp. 2292–2310

A MONOTONIC METHOD FOR THE NUMERICAL SOLUTION OF SOME FREE BOUNDARY VALUE PROBLEMS*

RAPHAÈLE HERBIN†

Abstract. This work presents an efficient monotonic algorithm for the numerical solution of the obstacle problem and the Signorini problems, when they are discretized either by the finite element method or by the finite volume method. The convergence of this algorithm applied to the discrete problem is proven in both cases.

In this work it is considered the OP given by

$$\begin{cases} u \in K = \{\phi \in H_0^1(\Omega) : \phi \leq \Psi \text{ on } \Omega\}, & \text{satisfying} \\ \int_\Omega \nabla u \cdot \nabla (v-u)\, dx \geq \int_\Omega f(v-u)\, dx, & \forall \phi \in K \end{cases}$$

where Ω is a bounded open polygonal subset of $\mathbb{R}^n$, with $d = 2$ or 3, $f \in L^2(\Omega)$ and $\Psi \in H^1(\Omega) \cap C(\Omega)$.

Gauss-Seidel for Reynolds model

$$a^n_{i-\frac{1}{2}}\,P^n_{i-1} - \left(a^n_{i-\frac{1}{2}} + a^n_{i+\frac{1}{2}}\right)P^n_i + a^n_{i+\frac{1}{2}}\,P^n_{i+1} = f^n_i$$

Algorithm 1: Gauss-Seidel for Reynolds cavitation model

Input: h^n: gap function, P^{n-1}: initial guess, *tol*: for stop criterion
Output: P^n pressure at time n
begin
- $k = 0$
- $P^{n,k} = P^{n-1}$
- **while** *change* $>$ *tol* **do**
  - $k = k + 1$
  - **for** $i = 1 \dots N$ **do**
    - $P^{n,k}_i = \frac{1}{a^n_{i-\frac{1}{2}} + a^n_{i+\frac{1}{2}}}\left(-f^n_i + a^n_{i-\frac{1}{2}}\,P^{n,k}_{i-1} + a^n_{i+\frac{1}{2}}\,P^{n,k-1}_{i+1}\right)$
    - $P^{n,k}_i = \max(0, P^{n,k}_i)$
  - **end for**
  - $change = \|P^{n,k} - P^{n,k-1}\|_\infty$
- **end while**
- return $P^{n,k}$

end

Convergence of Gauss-Seidel for the extremal formulation

Theorem

Algorithm 1 converges to the solution of the next equivalent problems

$$\mathbf{p}_h \geq 0 : \mathbf{p}_h^\intercal \mathbf{A}(\mathbf{v}_h - \mathbf{p}_h) \geq \mathbf{f}^\intercal(\mathbf{v}_h - \mathbf{p}_h), \forall \mathbf{v}_h \in \mathbb{R}_+^N \Leftrightarrow \min_{\mathbf{v}_h \in \mathbb{R}_+^N} \frac{1}{2}\mathbf{v}_h^\intercal \mathbf{A} \mathbf{v}_h - \mathbf{f}^\intercal \mathbf{v}_h$$

This is proved in "Optimization - Theory and Algorithms", Céa (1978).

Thus, we can compute the solution when $\mathbf{A}$ is given either by Finite Elements or Finite Volumes methods.

Reynolds model does not conserves mass

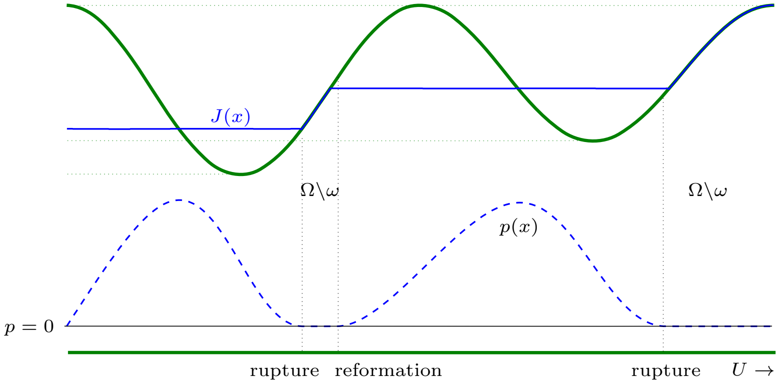

Mass-conservation at the pressurized zone

The steady-state Reynolds equation reads $\frac{\partial J}{\partial x} = 0$ only at ω. Cavitation modeling is a keystone when studying lubrication of tribological systems with textured surfaces, Priest et al., 2000; Ausas et al., 2007; Qiu et al., 2009.

Elrod-Adams model

Generalizing Reynolds equation: a saturation variable

Making use of JFO theory, Elrod et al., 1974, exposed a generalized Reynolds equation (elliptic in ω and hyperbolic at $\Omega \setminus \omega$) and an algorithm to solve it

$$\frac{\partial h\theta}{\partial t} = \nabla \cdot \left(\frac{h^3}{2} \nabla p - \frac{S}{2} h\theta \, \hat{\boldsymbol{e}}_1 \right) \qquad \text{and} \qquad p\,(1-\theta) = 0, \qquad \text{in } \Omega.$$

Existence results

- For the steady case ($h \in C^\infty$), in *"Nonlinear Variational Formulation for a Cavitation Problem in Lubrication"*, Bayada et al. (1982) proved the existence of a solution for the weak formulation.
- For the unsteady case, in *"Existence and numerical results of a transient lubrication problem with cavitation"*, El Alaoui et al. (2012) for $h \in C^1$ and a time interval $[0, T]$.

Both models predict different cavitated zones

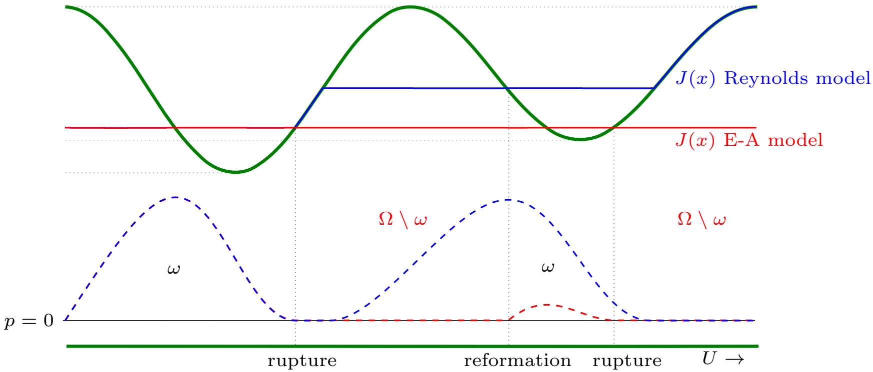

Experimental comparisons

In *"Direct observation of cavitation phenomenon and hydrodynamic lubrication analysis of textured surfaces"*, Zhang et al. (2012), is showed that Elrod-Adams predicts well cavitated zones obtained experimentally, while Reynolds model fails.

1D discretization for Elrod-Adams model

Finite Volumes

$$\frac{\partial h\theta}{\partial t} = \frac{\partial}{\partial x}\left(\frac{h^3}{2}\frac{\partial p}{\partial x} - \frac{S}{2}h\theta\right) \Rightarrow -\frac{h^3}{2}\frac{\partial p}{\partial x} + \frac{S}{2}h\theta \approx -\frac{1}{2}\frac{h_{i-1}^3 + h_i^3}{2}\frac{p_i - p_{i-1}}{\Delta x} + \frac{S}{2}h_{i-1}\theta_{i-1}$$

System to solve

$$a_{i-1}^n P_{i-1}^n - \left(a_{i-1}^n + a_i^n\right) P_i^n + a_i^n P_{i+1}^n = \gamma\left(h_i^n\theta_i^n - h_i^{n-1}\theta_i^{n-1} + \nu\left(h_i^n\theta_i^n - h_{i-1}^n\theta_{i-1}^n\right)\right)$$
$$P_i^n\left(1 - \theta_i^n\right) = 0$$

$$P_i^{n,k} = \frac{1}{a_{i-1}^n + a_i^n}\left(-\gamma\left(Q_i^{n,k-1} - Q_i^{n-1} - \nu\left(Q_i^{n,k-1} - Q_{i-1}^{n,k-1}\right)\right) + a_{i-1}^n P_{i-1}^{n,k} + a_i^n P_{i+1}^{n,k-1}\right) \tag{6}$$

$$\theta_i^{n,k} = \frac{1}{\gamma(1+\nu)}\left(\gamma\left(Q_i^{n-1} + \nu Q_{i-1}^{n,k}\right) + a_{i-1}^n P_{i-1}^{n,k} - \left(a_{i-1}^n + a_i^n\right) P_i^{n,k} + a_i^n P_{i+1}^{n,k-1}\right) \tag{7}$$

Algorithm 2: Gauss-Seidel for Reynolds equation with Elrod-Adams cavitation model

Input: h^n: gap function, $\left(P^{n-1}, \theta^{n-1}\right)$: initial guess, tol: for stop criterion
Output: P^n, θ^n pressure and saturation fields at time n resp.

```
begin
    k = 0
    P^{n,k} = P^{n-1}, θ^{n,k} = θ^{n-1}
    while change > tol do
        k = k + 1
        for i = 1 ... N do
            if P_i^{n,k-1} > 0 or θ_i^{n,k-1} == 1 then
                Compute P_i^{n,k} using (7)
                Complementary condition
            end if
            if P_i^{n,k} ≤ 0 or θ_i^{n,k} < 1 then
                Compute θ_i^{n,k} using (8)
                Complementary condition
            end if
        end for
        change = ||P^{n,k} - P^{n,k-1}||_∞ + ||θ^{n,k} - θ^{n,k-1}||_∞
    end while
    return (P^{n,k}, θ^{n,k})
end
```

Complementary condition (after computing $P_i^{n,k}$):

```
if P_i^{n,k} ≥ 0 then
    θ_k^{n,k} = 1
else
    P_i^{n,k} = 0
end if
```

Complementary condition (after computing $\theta_i^{n,k}$):

```
if θ_i^{n,k} < 1 then
    P_i^{n,k} = 0
else
    θ_i^{n,k} = 1
end if
```

Pure Squeeze motion

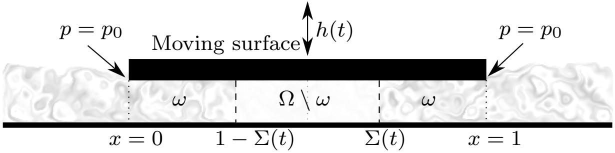

Figure : Pure Squeeze problem scheme.

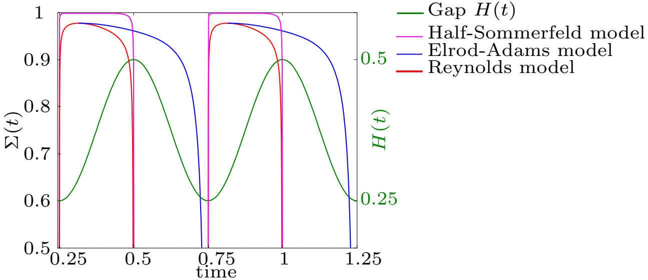

Figure : Comparison of cavitation models for a pure squeeze problem.

Used as a benchmark problem: Optasanu et al., 2000; Ausas et al., 2007.

A traveling pocket

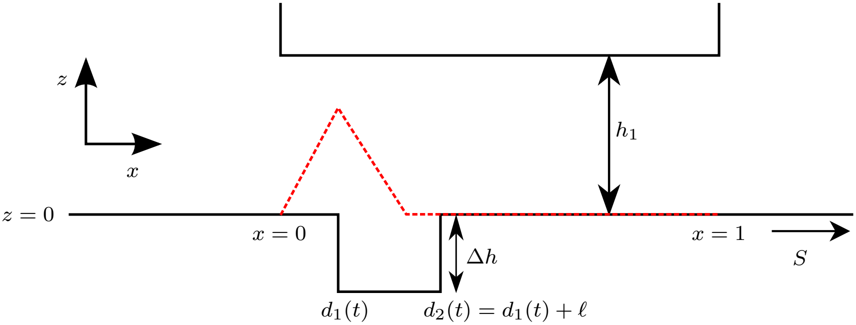

Figure : Traveling pocket scheme.

A traveling pocket: Reynolds model

Integrating we obtain:

$$p(d_1) = \frac{S\ell\, d_1 \Delta h}{d_1 h_2^3 + \ell h_1^3}$$

with $h_2 = \Delta h + h_1$.

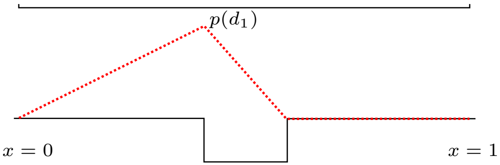

Figure : Ansatz.

For proving that, in fact, this is the solution we put it in the variational inequality

$$\int_0^1 h^3\, \partial_x p\, \partial_x(\phi - p)\, dx \geq S \int_0^1 h\, \partial_x(\phi - p)\, dx - 2 \int_0^1 (\phi - p)\, \partial_t h\, dx \qquad \forall \phi \in K,$$

with $K = \{\phi \in H_0^1(0,1) : \phi \geq 0\}$.

A traveling pocket: Elrod-Adams model

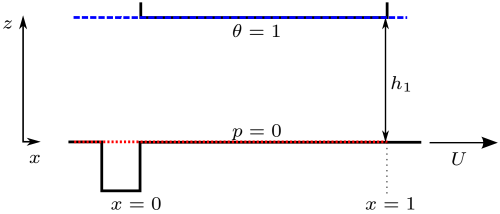

$$\frac{\partial}{\partial x}\left(\frac{h^3}{2}\frac{\partial p}{\partial x} - \frac{S}{2}h\theta\right) = \frac{\partial h\theta}{\partial t}, \text{ on } \Omega = [0,1]$$

For some point x, mass-conservation reads (V_x is the velocity of x),

$$J(x)_+ - J(x)_- = \left((h\theta)_+ - (h\theta)_-\right) V_x.$$

We obtain the next condition for $x = d_2$

$$\theta_-(d_2) = \frac{h_1}{h_2} + \frac{h_1^3 \partial_x p_+ - h_2^3 \partial_x p_-}{S h_2}.$$

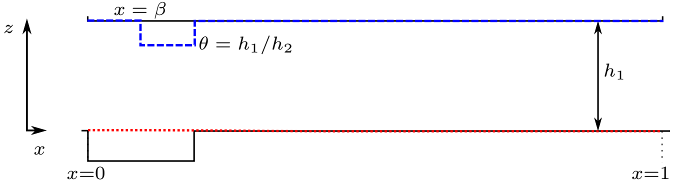

Analytic solution

Reynolds equation reads: $$\frac{\partial p}{\partial x} = \frac{C}{h^3} - \frac{S\Delta h}{h^3} H(x - d_1), \quad \text{on } \omega =]0, \beta[$$

The conditions $p(0) = p(\beta) = 0$ imply: $$p(d_1) = \frac{S(\beta - d_1)\, d_1 \Delta h}{d_1 h_2^3 + (\beta - d_1) h_1^3}$$

From mass-conservation we get: $$\frac{h_2^3}{2}\partial_x p_-(\beta) = h_2\,(\theta_+(\beta) - 1)\left(\beta' - \frac{S}{2}\right)$$

By characteristic lines $\theta_+(\beta) = h_1/h_2$ and $\beta' > S/2$ we obtain

$$\frac{d\beta}{dt} = \frac{S}{2}\left(1 + \frac{h_2^3}{h_2^3 + h_1^3(\beta/d_1 - 1)}\right)$$

Comparison of solutions

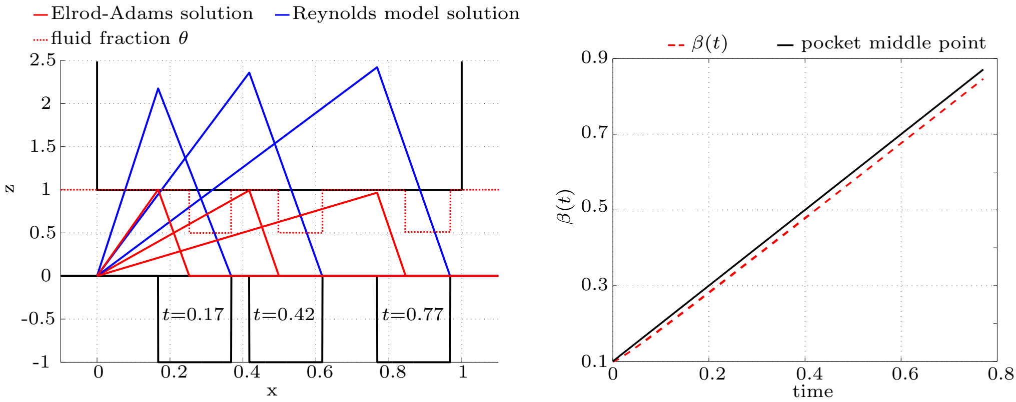

Figure : Left: Exact solutions for the pocket. Right: Evolution of the boundary $\beta(t)$.

Convergence rate

Comparisons at time $t = 0.77$

Parameters: $\Delta x = 1/N$, $\Delta t = \Delta x/(S/2)$ $(\nu = 1)$, $tol = 1 \times 10^{-7}$ and $N = 64, 128, 256, 512, 1024$.

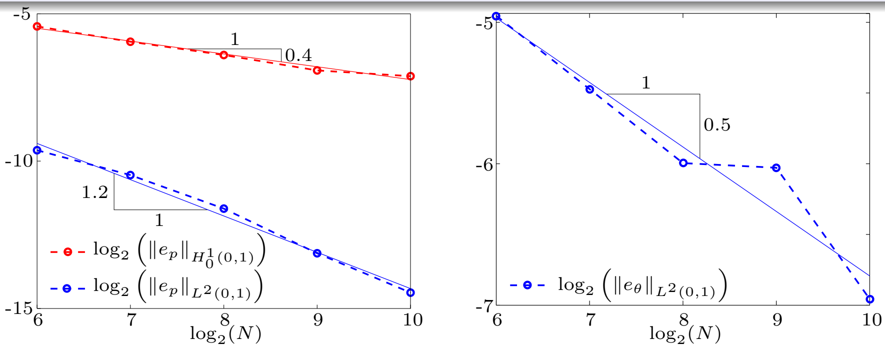

Figure : Pressure convergence in $L^2(0,1)$ and $H_0^1(0,1)$, and convergence for θ in $L^2(0,1)$.

Brezzi et al. (1977) proved convergence of order $\mathcal{O}(h)$ in $H_0^1(\Omega)$ for the OP.

Dynamical coupling

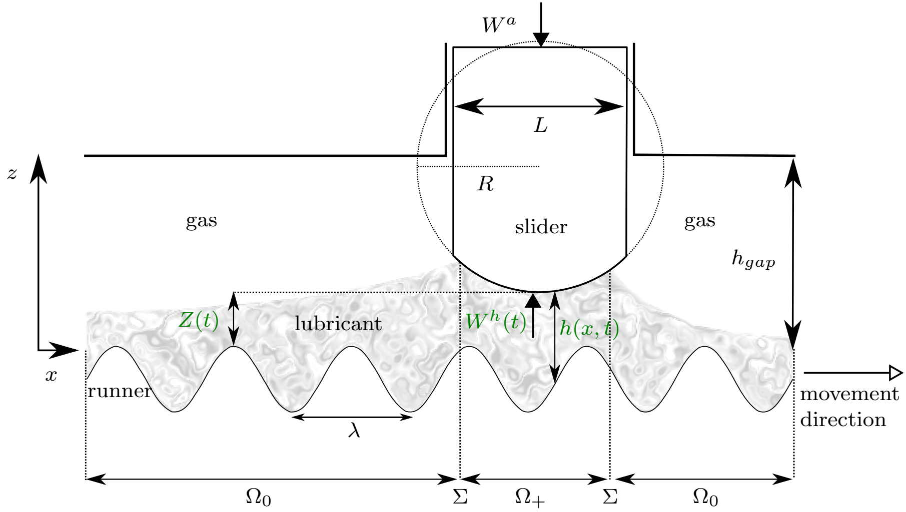

Figure : Textured surface and sliding bearing scheme.

Dynamical variables

$$h(x_1,t) = \begin{cases} h_a(x_1) + Z(t) - h_L(x_1 - U\,t), & a < x_1 < b \\ h_{gap} - h_L(x_1 - U\,t), & \text{rest of the domain,} \end{cases}$$

$$W^h(t) = \int_a^b p(x,t)\,dx,$$

$$m\,\frac{d^2 Z(t)}{dt^2} = -W^a + W^h(t).$$

Newmark Scheme

$$Z^n = Z^{n-1} + \Delta t\, U^{n-1} + \frac{\Delta t^2}{2}\frac{W^{h,n} - W_a}{m},$$

$$U^n = U^{n-1} + \Delta t\,\frac{W^{h,n} - W_a}{m}.$$

It is unconditionally stable on time, e.g., Geradin et al. (2015).

"Mass-conserving cavitation model for dynamical lubrication problems. Part I: Mathematical analysis.", Buscaglia et al., 2014.

Application: a slider bearing

1D numerical experiments

The runner is assumed to be sinusoidal with period λ and depth d

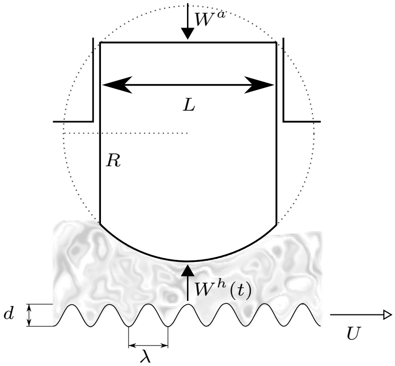

Figure : Numerical tests scheme.

Parameters

$$H = 10^{-6}\ \text{m} \qquad L = 10^{-3}\ \text{m}$$
$$U = 10\ \text{m/s} \qquad m = 4.8 \times 10^{-5}\ \text{kg}$$
$$W_0^a = 40\ \text{N/m} \qquad \text{R}/L = 32$$

$$\Omega = [0,\ 2] \qquad [a, b] = [0.5,\ 1.5]$$

$$h_L(x) = \ -d/2\,(1 - \cos(2\pi\, x/\lambda))$$
$$\text{N} = 512,\ \Delta t = 4 \times 10^{-3}.$$

"Texture-Induced cavitation bubbles and friction reduction in the Elrod-Adams Model", Checo et al., 2015.

Application: a slider bearing

Quantities of interest

$$F = \int_a^b \left(\frac{\mu U g(\theta)}{h} + \frac{h}{2}\frac{\partial p}{\partial x} + p\frac{\partial h_L}{\partial x} \right) dx.$$

So the friction coefficient is given by

$$f(t) = \frac{H}{6L}\frac{\hat{F}}{\hat{W}_a}, \qquad \overline{f} = \frac{1}{\lambda}\int_T^{T+\lambda} f(t)dt.$$

The minimal clearance is calculated as

$$C_{\min} = \inf_{t \in [T, T+\lambda]} \left(\inf_{x \in]a,b[} h(x,t) \right).$$

"Moving textures: Simulation of a ring sliding on a textured liner", Checco et al., 2014.

Friction chart for R = 32

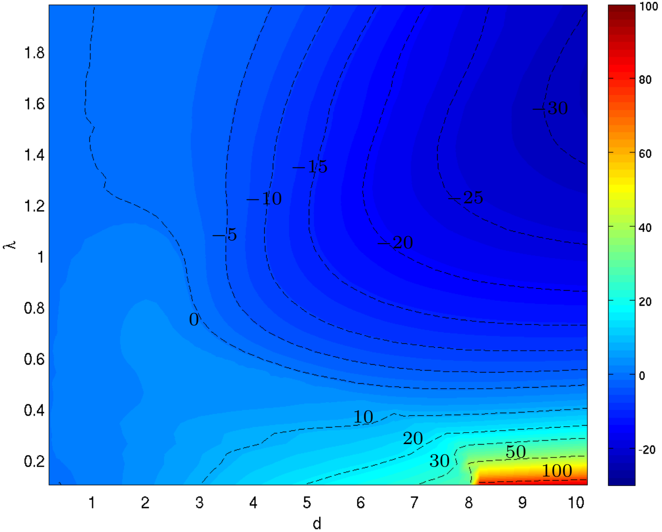

$\lambda \in [0.1, 1.98]$, $\Delta\lambda = 0.04$. $d \in [0.2, 10.2]$, $\Delta d = 0.2$ ($48 \times 51 = 2448$ simulations).

Clearance chart for R = 32

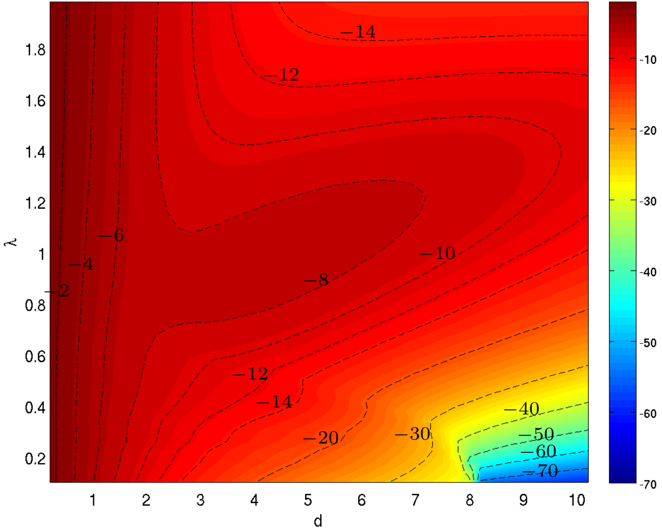

$\lambda \in [0.1, 1.98]$, $\Delta\lambda = 0.04$. $d \in [0.2, 10.2]$, $\Delta d = 0.2$ ($48 \times 51 = 2448$ simulations).

Two interesting observations ($R = 32$, $\lambda = 0.1$, $d = 8.2$)

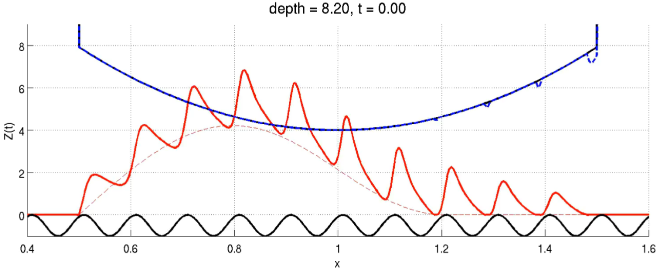

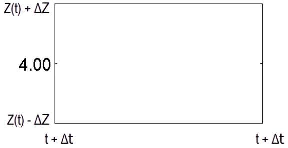

$\Delta t = 0.9$, $\Delta Z = 0.005$

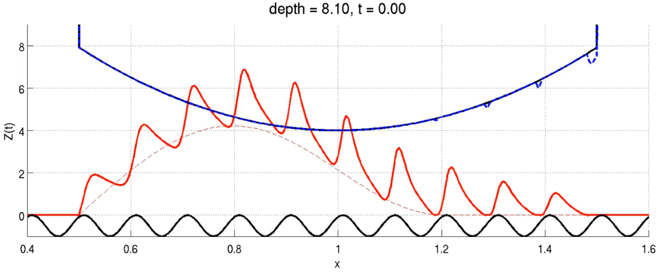

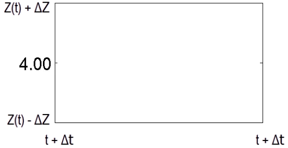

Stability on $\Delta t = \nu\,\Delta x/(S/2)$

Selected case and numeric parameters

We take $d = 4.0$, $\lambda = 0.2$, $\nu \in \{0.5, 1.0, 2.0, 4.0, 8.0\}$ and $\mathrm{N} \in \{128, 256, 512, 1024\}$. The calculations are done once the stationary state is reached.

N\\ν	0.5	1.0	2.0	4.0	8.0
2^6	4.97	8.68	17.4	28.1	20.4
2^7	2.28	3.84	7.74	16.6	28.5
2^8	1.00	1.52	3.23	7.21	16.2
2^9	0.36	0.58	1.09	2.85	6.85
2^{10}	0.00	0.06	0.20	0.63	2.32

Table : Convergence in $\bar{f}$ (%).

N\\ν	0.5	1.0	2.0	4.0	8.0
2^6	3.43	5.04	7.29	3.84	4.21
2^7	1.30	1.85	3.38	5.84	2.66
2^8	0.48	0.59	1.03	2.47	5.02
2^9	0.18	0.18	0.24	0.61	1.99
2^{10}	0.00	0.08	0.19	0.27	0.08

Table : Convergence in $C_{\min}$ (%).

Future work

Unstructured meshes: Discontinuous Galerkin (DG)

The adopted method has poor mesh flexibility and low convergence order. Higher order methods based on continuous interpolants cannot be applied because of the spontaneously-generated discontinuities at cavitation boundaries. DG Methods and DG-based FVM overcome these issues for elliptic problems (Codina et al., 2013) and hyperbolic problems (Cockburn, 2001).

Elrod-Adams extentions: transport velocity in the cavitated zone

To extend Elrod-Adams for allowing transport greater than $S/2$ is a challenging problem, lack of uniqueness of solution is one of its difficulties; and a *front-capturing* algorithm is not available yet. Some efforts on this issue can be found in Checo Ph.D. Thesis.

Boundary conditions for pressure

Current cavitation models only admit a constant cavitation pressure equal to the surrounding pressure. This is being questioned by some researchers (Shen et al., 2013) and is a source of inaccuracy. At some instants in the engine cycle the pressure difference between both sides of the ring pack can reach 100[atm].

Future work

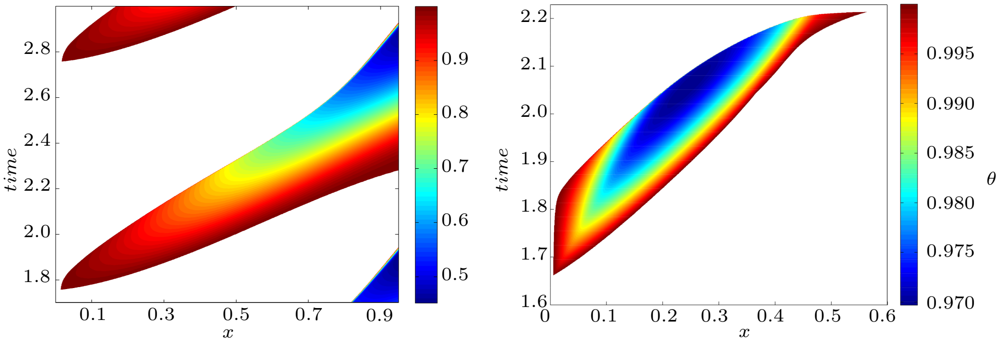

Figure : Cavitation bubbles for two different sinusoidal textures. Left: R=32, $d = 5$. Right: R= 256, $d = 0.75$.

$$L = 1[\text{mm}],\ \lambda = 1.\ N = 4096,\ \Delta x = 4.88 \times 10^{-5}[\text{cm}],\ \nu = 0.5.$$

Future work

For the left border we write the function $x_e : [t_0, t_f] \to [a,b] \subset \Omega$ and adjust a curve like

$$x_e(t) \approx C\,(t-t_0)^{\alpha+1},\; t_0 < t < t_\epsilon = t_0 + \epsilon \Rightarrow \left.\frac{dx_e}{dt}\right|_{t_0} \approx C\,(\alpha+1) \lim_{t\to 0^+} t^\alpha .$$

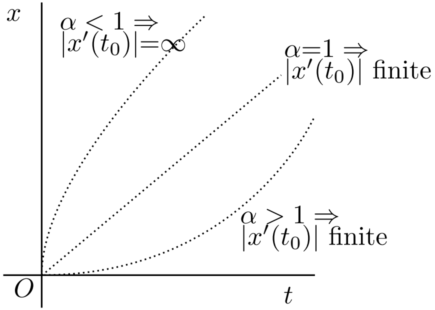

Figure : Curves $\approx t^{\alpha+1}$ for different types of α, with $O = (x_e(t_0), t_0)$.

Future work

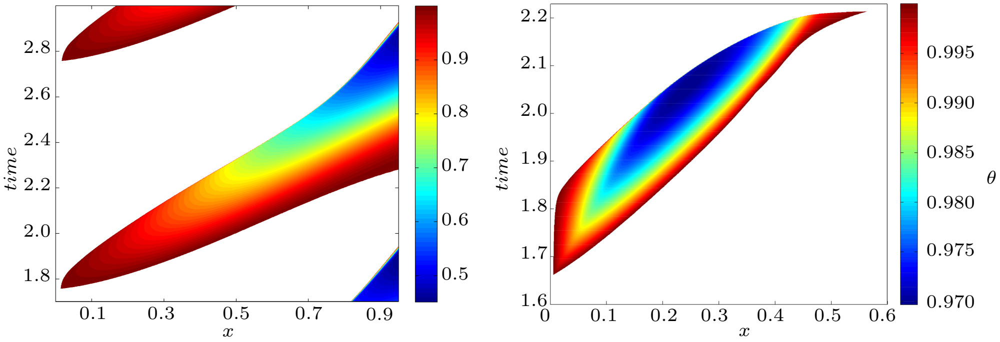

Figure : Cavitation bubbles for two different sinusoidal textures. Left: R=32, $d = 5$. Right: R= 256, $d = 0.75$.

Thanks for your attention